

Symbiotic Innovation in the Oxymonad *Streblomastix strix*

BRIAN S. LEANDER and PATRICK J. KEELING

Canadian Institute for Advanced Research, Program in Evolutionary Biology, Departments of Botany and Zoology, University of British Columbia, Vancouver, BC, V6T 1Z4, Canada

ABSTRACT. *Streblomastix strix* is an enigmatic oxymonad found exclusively in the hindgut of the damp-wood termite *Zootermopsis*. *Streblomastix* has a number of unusual morphological characters and forms a complex but poorly understood symbiosis with epibiotic bacteria. Here we described the ultrastructure of *S. strix*, with emphasis on the axial cytoskeleton and cell-cell associations, in its normal state and when treated with antibiotics. In untreated cells, epibiotic bacteria were orderly arranged end-to-end on six or seven longitudinal vanes, giving *S. strix* a stellate appearance in transverse section. The epibiotic bacteria were unusually long bacilli of at least three different morphotypes. Bacteria adhered to the oxymonad host by distinct cell-cell junctions that protruded between the poles of adjacent epibiotic bacteria. Treating termites with the antibiotic carbenicillin led to the loss of most (but not all) of the bacteria and the transformation of *S. strix* from a long slender cell to a teardrop-shaped cell, where the axostyle was compacted and became bifurcated near the posterior end.

Key Words. Electron microscopy, epibiotic bacteria, excavates, oxymonads, symbiosis, termites, ultrastructure.

OXYMONADS are a relatively diverse and poorly understood group of flagellates found exclusively in low-oxygen environments within animals, predominantly the guts of wood-eating termites and cockroaches. These insect guts are home to a diverse community of bacteria and eukaryotic flagellates (typically parabasalids and oxymonads) that facilitate the degradation of cellulose into absorbable compounds, such as acetate. Most of the flagellates play important roles in maintaining this symbiotic system, but some hindgut inhabitants, including many oxymonads, may be ‘hitchhikers’, in that they do not contribute to cellulose degradation but do exploit the resulting pool of nutrients (Cleveland 1925).

The best cytoskeletal synapomorphy for oxymonads is a distinctive ‘axostyle’ composed of parallel sheets of microtubules that extend longitudinally and may undulate rapidly inside the cell (Brugerolle and Lee 2000; Patterson 1999). The flagellar apparatus consists of four or more axonemes and associated basal bodies arranged in two pairs and connected by a ‘preaxostylar lamina’ that serves as a nucleation site for the microtubules of the axostyle (Brugerolle and Lee 2000). A thin veil of microtubules, called the ‘pelta’, usually arises from one of the basal bodies, supports the anterior surface of the cell and surrounds the anterior region of the nucleus. The flagella may be oriented posteriorly or anteriorly, and in the former case may be physically attached to the cell surface (Bloodgood et al. 1974; Hollande and Carruette-Valentin 1970).

Oxymonads lack traditionally recognizable mitochondria and Golgi bodies (Brugerolle 1991; Cavalier-Smith 1983, 1987). However, absence of these structures is almost certainly secondary, because the closest relative to oxymonads in molecular phylogenies is *Trimastix* (Dacks et al. 2001; Keeling and Leander 2003; Moriya et al. 2003; Stingl and Brune 2003), which possesses standard Golgi bodies and mitochondrion-like structures (putative hydrogenosomes) (Brugerolle and Patterson 1997; O’Kelly et al. 1999; Simpson et al. 2000). Moreover, *Trimastix* is allied on ultrastructural grounds with several other groups of mitochondrion-bearing and Golgi-bearing eukaryotes having so-called ‘excavate type’ morphologies (Simpson et al. 2000, 2002). Therefore, it is anticipated that vestiges of mitochondria and Golgi bodies will eventually be discovered in oxymonads.

The cell surface of oxymonads almost invariably includes specialized extracellular structures involved in the attachment of epibiotic bacteria (Rother et al. 1999). These eukaryote-bacterial associations and their associated cytoskeletal proper-

ties are poorly understood at even the purely descriptive level in most oxymonads. Accordingly, we have investigated the ultrastructure of an enigmatic oxymonad *Streblomastix strix*, which lives in two species of *Zootermopsis*, damp-wood termites of northwest North America. Early studies using light microscopy established that *S. strix* are relatively rigid, spindle-shaped cells with four anterior flagella and a long, twisted thread-like nucleus. Cells are usually 20–50 µm long and 6–10 µm wide. They can reach over 530 µm in length as aberrant whip-like forms when the termites are starved (Kidder 1929; Kofoid and Swezy 1919). Some cells possess a ‘holdfast’, which is an extension of an anterior knob that functions to attach cells to the lining of the termite hindgut (Brugerolle and Lee 2000; Kidder 1929). A few scattered electron micrographs have demonstrated that *S. strix* has a stellate cross-sectional morphology and is almost completely enveloped by a dense community of epibiotic bacteria (Dexter-Dyer and Khalsa 1993; Hollande and Carruette-Valentin 1970; Keeling and Leander 2003; Yamin 1979).

Here we have investigated the fundamental ultrastructural properties of *S. strix* in its normal state, in addition to ultrastructural modifications associated with a drug treatment that disrupts the epibionts (Dexter-Dyer and Khalsa 1993). We examined both treated and untreated cells with scanning and transmission electron microscopy, paying particular attention to epibiont-host cell interactions and the fundamental organization of the axial cytoskeleton.

MATERIALS AND METHODS

Collection of organisms. Damp wood termites (*Zootermopsis angusticollis*) were collected from the local forests of coastal British Columbia (Pacific Spirit Park, Vancouver, Canada) and maintained on moistened wood. Contents of the termite hindgut were squeezed into a pool of Trager medium U (Trager 1934). *Streblomastix strix* was among the most abundant protozoan components in these suspensions.

Light microscopy. Cells observed with DIC light microscopy were suspended in Trager medium U, fixed in 1% (v/v) glutaraldehyde, and secured under a cover slip with VALAP [1 vaseline: 1 lanolin: 1 paraffin; (Kuznetsov et al. 1992)]. Images were produced with a Zeiss Axioplan 2 Imaging microscope connected to a Q-Imaging, Microimager II, black and white digital camera.

Scanning electron microscopy. A small vol. (10 ml) of cells suspended in Trager medium U was transferred into a Petri dish containing filter paper mounted on the inner surface of the lid. The filter paper was saturated with 4% OsO₄ and placed over the dish. The cells were fixed by OsO₄ vapors for 30 min before adding six drops of 4% (w/v) OsO₄ directly to the medium.

Corresponding Author: B. Leander—Telephone number: 604-822-2474; FAX number: 604-822-6089; E-mail: bleander@interchange.ubc.ca

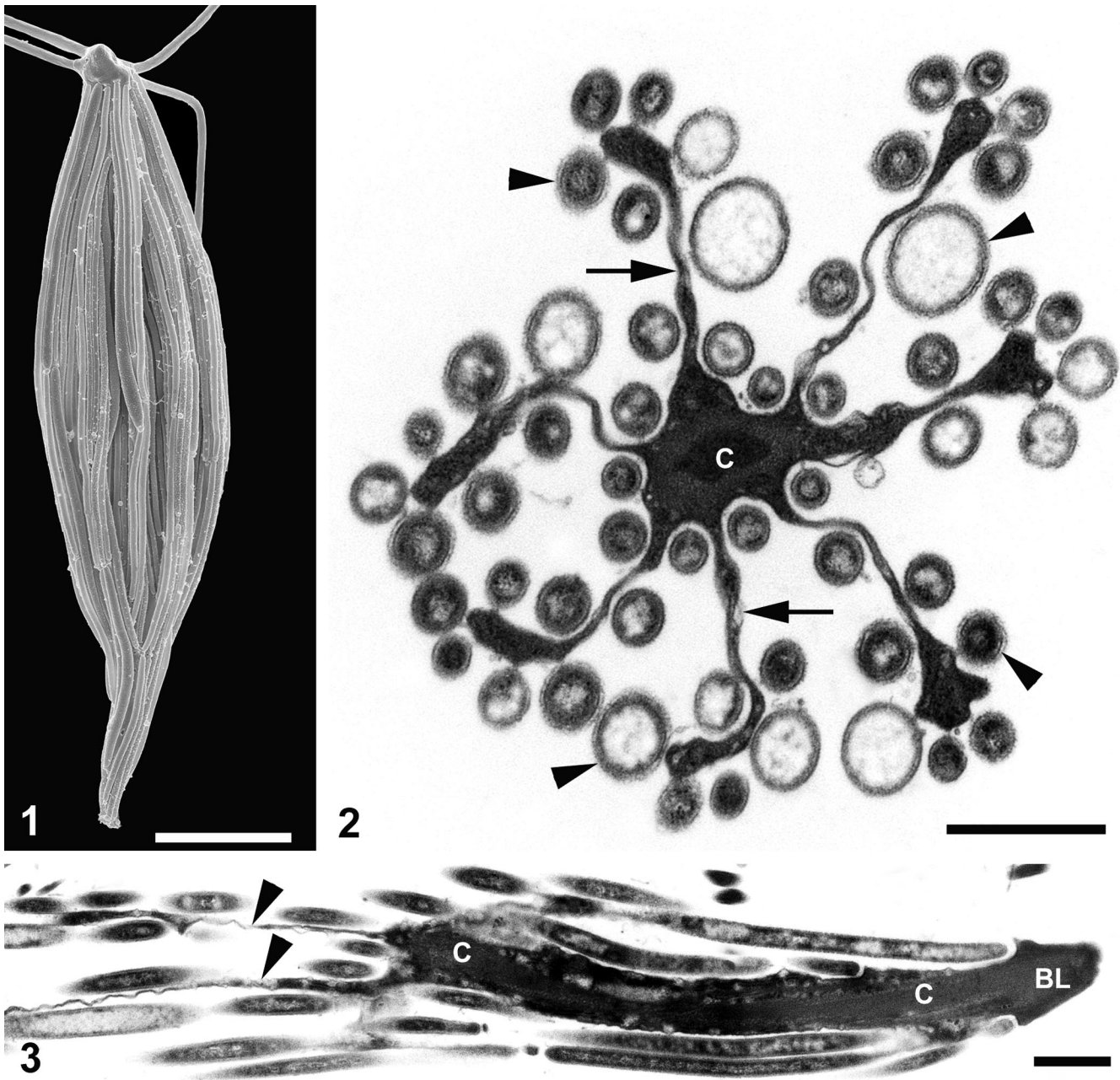


Fig. 1-3. General morphology of *Streblo mastix strix*. **1.** SEM of a spindle-shaped cell showing four anterior flagella and a dense community of elongated epibiotic bacteria over the host cell surface (Bar = 5 μm). **2.** TEM transverse section showing the stellate morphology of the host cell. The host was organized as a central core (c) with seven thin vanes radiating outward (arrows). Seven to ten epibiotic bacteria with distinctive morphotypes were clustered around each vane (arrowheads) (Bar = 1 μm). **3.** TEM tangential section through the anterior region of *S. strix* showing the naked anterior bulb of the cell (BL), central core (c), and longitudinal continuation of the thin vanes (arrowheads) (Bar = 1 μm).

After an additional 30 min of fixation, cells were transferred onto a 5- μm polycarbonate membrane filter (Corning Separations Div., Acton, MA), dehydrated with a graded series of ethyl alcohol, and critical point-dried with CO_2 . Filters were mounted on stubs, sputter-coated with gold, and viewed under a Hitachi S4700 Scanning Electron Microscope. Some SEM images were presented on a black background using Adobe Photoshop 6.0 (Adobe Systems, San Jose, CA).

Transmission electron microscopy. Cells suspended in Trager medium U were concentrated in Eppendorf tubes by slow centrifugation. Pellets of cells were prefixed with 2% (v/v) glu-

taraldehyde in 0.1 M cacodylate buffer, pH = 7 and 0.4% NaCl at 4 $^\circ\text{C}$ for 1 h. Cells were washed twice in 0.1 M cacodylate buffer and 0.4% NaCl before post-fixation in 1% (w/v) OsO_4 , 0.4% NaCl and cacodylate buffer for 1 h. Cells were dehydrated through a graded series of ethyl alcohols, infiltrated with acetone-resin mixtures (pure acetone, 1:3, 1:1, 3:1, pure resin), and embedded in pure resin. Blocks were polymerized at 60 $^\circ\text{C}$ and sectioned with a diamond knife on a Leica Ultracut Ultra-Microtome. Thin sections were post-stained with uranyl acetate and lead citrate and viewed under a Hitachi H7600 Transmission Electron Microscope.

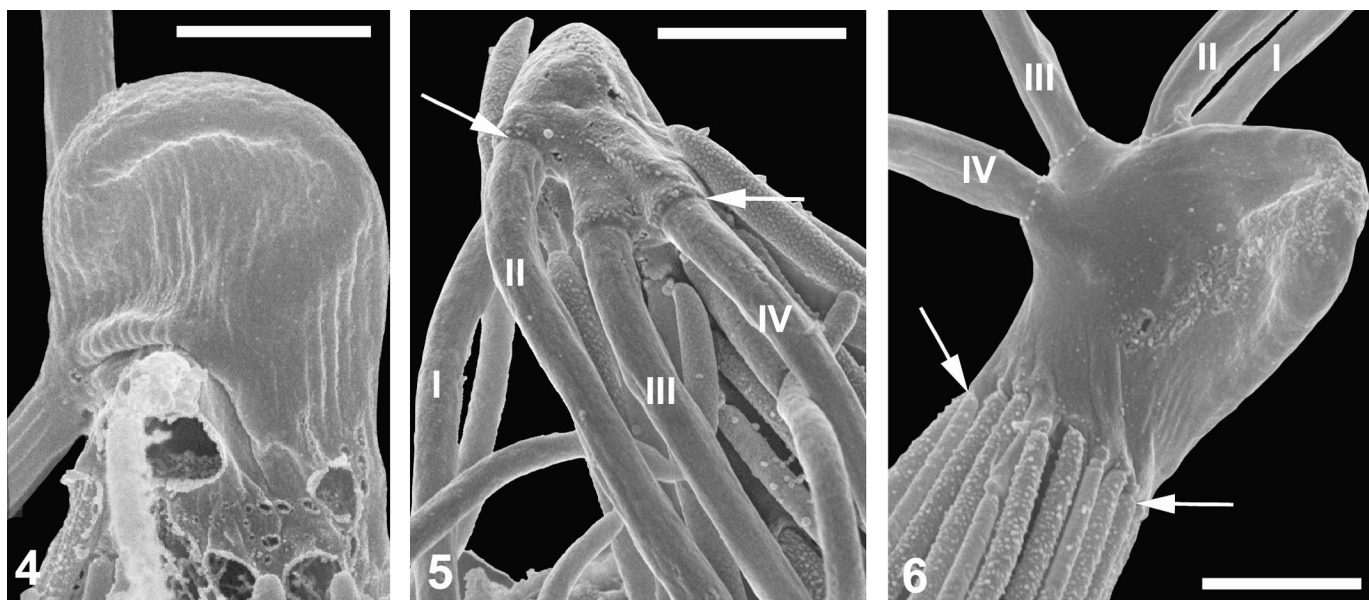


Fig. 4–6. Anterior end of *Streblomastix strix*. 4. SEM showing the microtubules of the pelta underlying the naked anterior end of the cell, which was evident as fine longitudinal striations (Bar = 1 μ m). 5. Ventral SEM of the anterior end of the cell showing the four flagella (I, II, III, IV) oriented posteriorly and the junctions between axonemes and basal bodies (arrows) (Bar = 1 μ m). 6. Lateral SEM of the anterior end of the cell highlighting the ‘two-paired’ organization and anterior orientation of the four flagella. A distinctive ‘collar’ of attached epibiotic bacteria at the base of the anterior end of the cell (arrows) was always present (Bar = 1 μ m).

Antibiotic treatment. Termites were isolated in small Petri dishes and maintained on moistened filter paper. The antibiotic carbenecillin was added to the filter paper by protocols described previously (Dexter-Dyer and Khalsa 1993).

RESULTS

General morphology. Individuals of *S. strix* were relatively rigid, spindle-shaped cells usually 20–50 μ m long with a dense community of elongated epibiotic bacteria over the cell surface (Fig. 1). Transverse sections through the mid-region of cells revealed a stellate organization, where the host cell was reduced to a central core with six or seven vanes radiating outward (Fig. 2). The vanes were very thin, ranging from 0.05 μ m in width near the middle to 0.5 μ m in width near the distal edge, and were continuous along the entire length of the cell (Fig. 3, 14A). Approximately 8–10 epibiotic bacteria, some of which were deeply positioned near the central core, were clustered around each of the vanes (Fig. 2). The posterior end of the cell tapered to a sharp point (Fig. 1).

The anterior end of the cell was completely devoid of epibiotic bacteria, forming a naked bulb (Dexter-Dyer and Khalsa 1993) defined by a distinctive collar of bacterial attachment sites (Fig. 3–6). The anterior end of the cell was supported by microtubules of the pelta, which were visible with the TEM and SEM (Fig. 3, 4). Four flagella arranged as two pairs were inserted subapically and were directed posteriorly when cells were swimming forward (Fig. 5) and anteriorly when cells were swimming backward (Fig. 6). The orientation of the basal bodies within the anterior end of the cell changed with the orientation of the flagella (cf. Fig. 5, 6). Cells typically swam forward while rotating counter-clockwise.

The axial cytoskeleton. The post-flagellar cytoskeleton consisted of microtubules from two principal components: the axostyle and the pelta. The microtubules of the pre-nuclear axostyle (syn. ‘rhizoplast’, Kidder 1929) were arranged in eight to ten parallel rows that were characteristic of other oxymonads (Brugerolle and Lee 2000) (Fig. 7). Helically arranged micro-

tubules of the pelta encircled the pre-nuclear axostyle and extended posteriorly to about one-fourth of the cell (Fig. 7, 12, 14B). A long thread-like nucleus was completely enveloped by a cytoskeletal cylinder comprised of a single row of axostylar microtubules (Fig. 8–10, 14B). The anterior end of the nucleus was also encapsulated by a second outer row of microtubules derived from the descending pelta (Fig. 8, 14B). Multiple rows of converging microtubules (2–3) were present around the tapering posterior end of the nucleus (Fig. 10, 14B). Once the nucleus terminated completely, the axostyle consisted of a relatively loose bundle of roughly 30 microtubules (Fig. 11, 14B). Microtubules were absent in the vanes and the absolute posterior end of the cell (Figs. 2, 13, 14B).

Cytoplasmic features. The cytoplasm of the host was very dense and contained intracellular bacteria and several membranous structures of undetermined homology and function (Fig. 2, 7–11, 31, other data not shown). The density (darkness) of the cytoplasm is inferred to be a peculiar property of *S. strix* rather than merely a chemical fixation artifact, as the cells of *Trichonympha* (hypermastigote) and *Trichomitopsis* (trichomonad) in the same TEM preparation had cytoplasm densities that were typical of other eukaryotic cells. Large vacuoles were occasionally adjacent to the central core (not shown), and distinctive multilayered membranous structures were observed both inside and outside the hollow cylinder of axostylar microtubules (Fig. 8). Intracellular bacteria (either endosymbionts or food) were present within vacuoles in the central core and in the vanes (not shown).

Episymbiotic bacteria and cell-cell junctions. Except for the anterior end of the cell, the surface of *S. strix* was completely covered with elongated bacteria that ranged from 5–10 μ m in length. Under normal conditions, hosts are estimated to harbor approximately 100–200 bacteria over the cell surface (e.g. 7 vanes multiplied by 9 bacteria per vane multiplied by 2–3 bacteria aligned end-to-end along the total length of the host cell = 126–189 bacteria). About 40% of the surface area

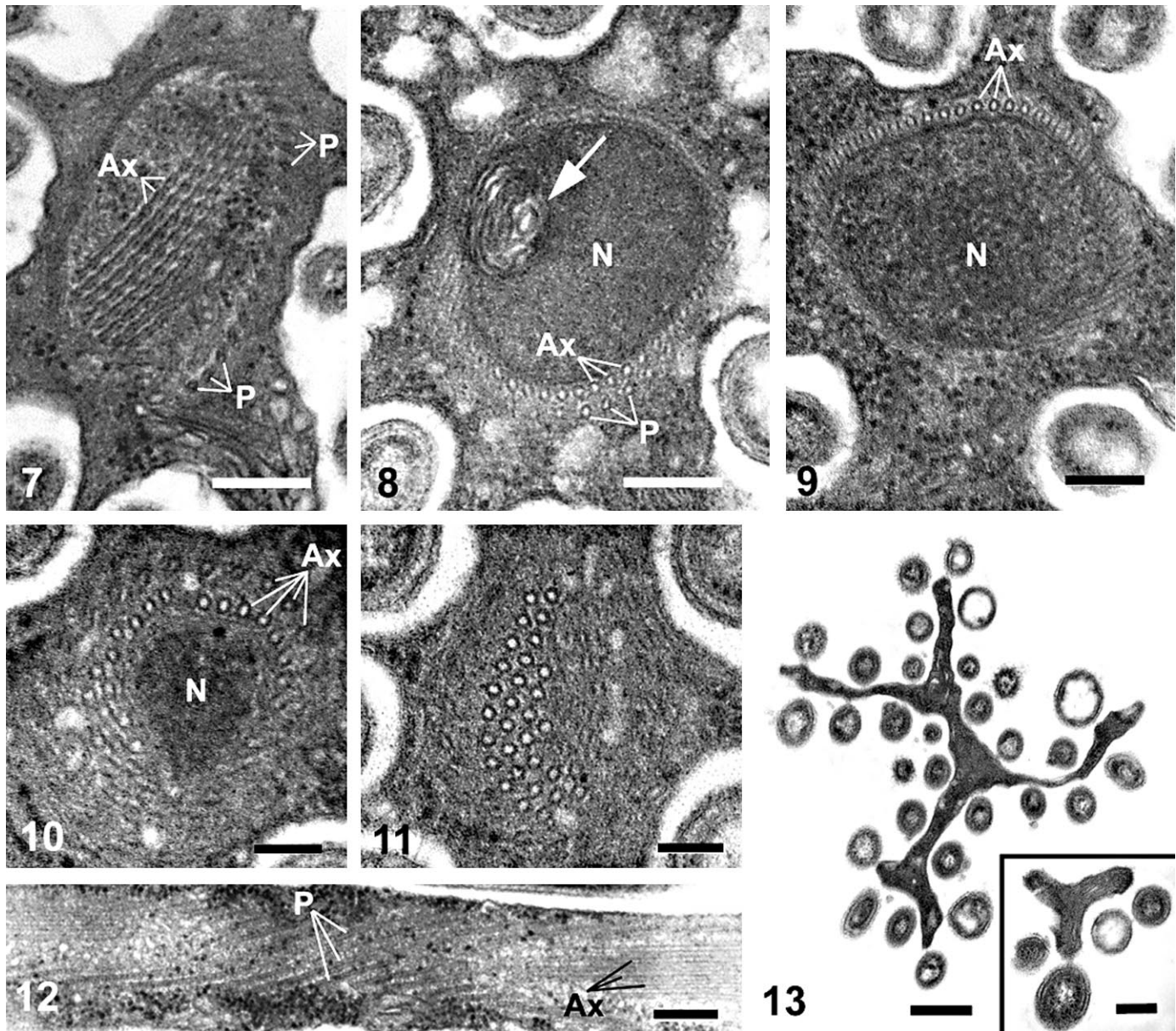


Fig. 7–13. TEM sections through the central core of *Streblomastix strix* showing the nucleus and microtubules of the axial cytoskeleton (anterior end of cell = upper left; posterior end of cell = lower right). **7.** Anterior transverse section showing the microtubules of the ‘pelta’ (P) surrounding the distinctive microtubular rows of the axostyle (Ax) (Bar = 0.2 μm). **8.** Transverse section through an anterior region of the long threadlike nucleus (N) illustrating the double row of microtubules formed by the axostyle (Ax) and pelta (P). The arrow marks a multi-membranous structure of undetermined homology and function (Bar = 0.2 μm). **9.** Transverse section through a mid-region of the nucleus (N) showing a single row of microtubules formed by the axostyle (Ax) (Bar = 0.2 μm). **10.** Transverse section through a posterior region of the nucleus (N) showing multiple rows of microtubules formed by the axostyle (Ax) (Bar = 0.2 μm). **11.** Transverse section showing the microtubular configuration of the post-nuclear axostyle (Bar = 0.2 μm). **12.** Longitudinal section of the anterior central core showing microtubules of the pelta (P) helically arranged around the microtubules of the pre-nuclear axostyle (Ax) (Bar = 0.2 μm). **13.** Posterior transverse section showing the absence of microtubules (Bar = 0.5 μm). Inset: Transverse section through the posterior terminus of the cell (Bar = 0.2 μm).

of each cross-section was attributable to bacteria, assuming that the bacteria, the central core of *S. strix*, and the tips of each vane were circles of known radius and the remaining parts of each vane were elongated rectangles (see Fig. 2).

A close examination of the episymbionts suggested that there were at least three different morphotypes, which differed in size, surface morphology, and cytoplasmic appearance (Fig. 2, 15). Two of the morphotypes had a maximum diameter of 0.5 μm , and the third morphotype was 1.5–2 \times larger at about 0.7–

1 μm . The three morphotypes differed in surface morphology, which was the main criterion for discrimination (Fig. 15). The episymbionts were fixed along their lateral surfaces to distinct swellings in the host cell by glycocalyx-like material (Fig. 16), and in most cases, the posterior-most bacterium was cupped by the cytoplasm of the host (Fig. 17). Septa between dividing epibiotic bacteria (Fig. 18, 19) and connecting pili between adjacent bacteria (of the same morphotype) were occasionally observed (Fig. 20). Each terminus of the bacteria was attached by

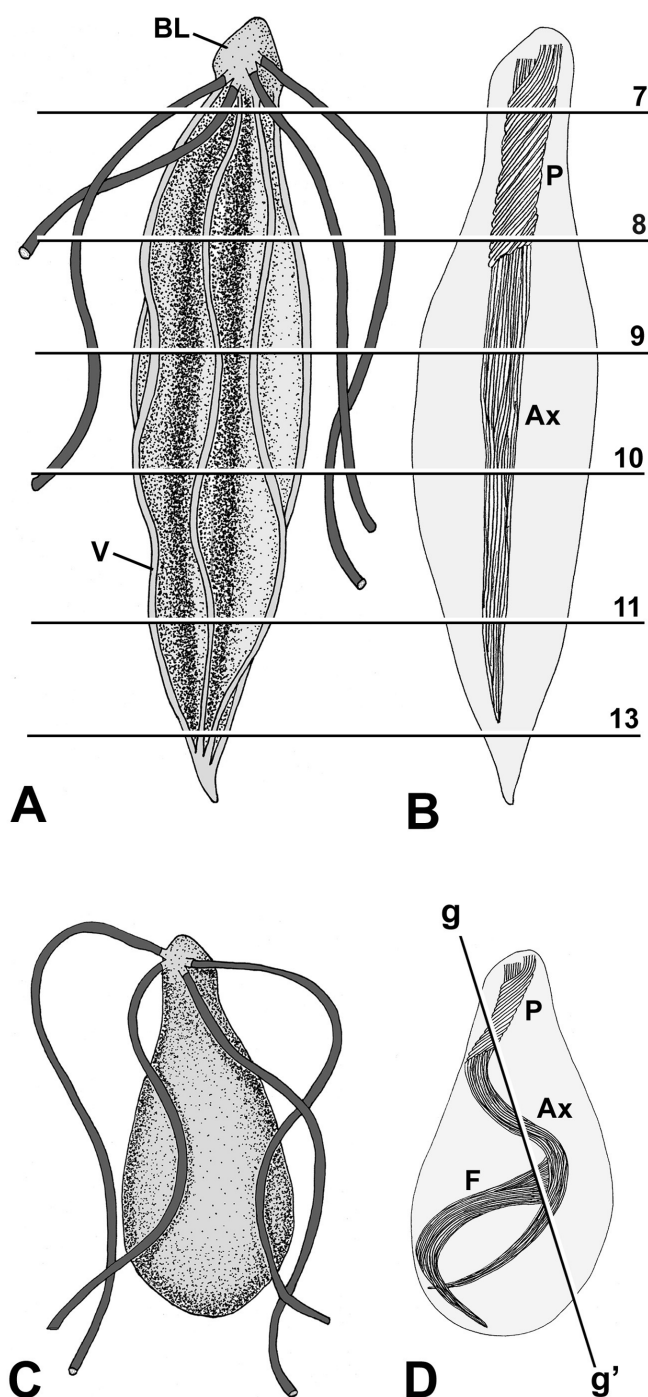


Fig. 14. Conceptual drawings of the cell surface of *Streblomastix strix* with the bacteria removed (A), the axial cytoskeleton of a 'normal' or untreated cell (B), the host cell surface following treatment with carbenecillin (C), and the axial cytoskeleton of a cell treated with carbenecillin (D). Numbers on transverse sections correspond to the figures presented on the previous plate. Oblique section $g-g'$ corresponds to Fig. 30 and Fig. 32. Note that the thread-like nucleus is contained within the mid-region of the hollow cylindrical axostyle (sections 8, 9 and 10). Ax, axostyle; BL, anterior bulb; F, fan of microtubules; P, pelta; V, vane.

the glycocalyx-like material to distinctive protuberances or 'knobs' (syn. 'spherical structures', Yamin 1979) derived from the host cell (Fig. 15, 21–23). These knobs had a biconcave morphology that accommodated the termini of two different bacteria oriented along the same longitudinal axis (Fig. 15, 22). The knobs were ultrastructurally simple, being comprised of dark-staining layers directly subtending the plasma membrane of the bacterial attachment sites (Fig. 22, 23).

Ultrastructure of carbenecillin-treated cells. The general morphology of *S. strix* changed significantly following treatment with the antibiotic carbenecillin. Transitional stages between untreated cells and treated cells had a reduced stellate structure and a greatly increased cell volume, suggesting a breakdown in osmoregulation (Fig. 24, 25). These cells possessed numerous bacteria that were attached to the host by only one terminus, thus a greater proportion of the cell surface was exposed (Fig. 24). The surface of the host retained many abandoned knobs (attachment sites) and the termini of remaining bacteria often lacked an attachment site (Fig. 28, 29). Treated cells were smaller and teardrop-shaped, and retained only a few laterally attached bacteria of a single morphotype (Fig. 14C, 26, 27). The abandoned attachment sites present on transitional stages and all indications of the original stellate morphology completely disappeared in the treated cells (Fig. 26, 27). After 3 to 4 days of carbenecillin treatment, cells of *S. strix* were very few in number and eventually disappeared altogether. Bacteria were also scarce, but *Trichonympha* and *Trichomitopsis* appeared to be unaffected by the carbenecillin treatment.

Both treated and untreated cells contained intracellular bacteria and an axial cytoskeleton surrounding the nucleus (Fig. 30, 31, 34). However, the density of the cytoplasm changed significantly in treated cells from the very dark appearance seen in untreated cells to a lighter consistency more typical of other eukaryotic cells in the preparation (Fig. 25, 27, 31–35). Treatment also induced significant changes in the structure of the axostyle, which was transformed from a long straight structure to a shorter undulating structure, much smaller in diameter, and possessing a 'fan' of microtubules that branched away from the main axis near the mid-section of the cell (Fig. 14D, 30, 32–35). The morphology of the axial cytoskeleton near the anterior end of the cell, which includes microtubules of the pelta, was essentially identical to that in untreated cells (Fig. 7, 31, 35). As expected, the axostyle in transitional stages of bacterial detachment was more robust than the axostyle of treated cells.

DISCUSSION

Functional morphology. *Streblomastix strix* is covered with a community of symbiotic bacteria. The elongated spindle shape and radiating vanes of *S. strix* are likely adaptations for maximizing the surface contact area for the attachment of these bacteria. This view is supported by the convergently acquired stellate architectures present in other unrelated gut symbionts, such as the cockroach-inhabiting hypermastigote *Lophomonas striata* (Beams et al. 1960). The central core of *S. strix* is almost entirely filled by an axostyle that encircles a long thread-like nucleus, a configuration that is likely a structural constraint of streamlining. The axostyle of most oxymonads is quite robust and motile (Bloodgood and Miller 1974; Brugerolle and König 1997; McIntosh 1973). However, the axostyle of *S. strix* is very reduced and almost completely rigid, which certainly helps stabilize the attached bacteria on the cell surface. The pelta, which in other oxymonads is confined to the very anterior end of the cell (Brugerolle 1991; Brugerolle and Lee 2000), extends posteriorly to about one-fourth of the cell length in *S. strix* providing additional structural integrity to the relatively long pre-nuclear axostyle (syn. 'rhizoplast', Kidder 1929).

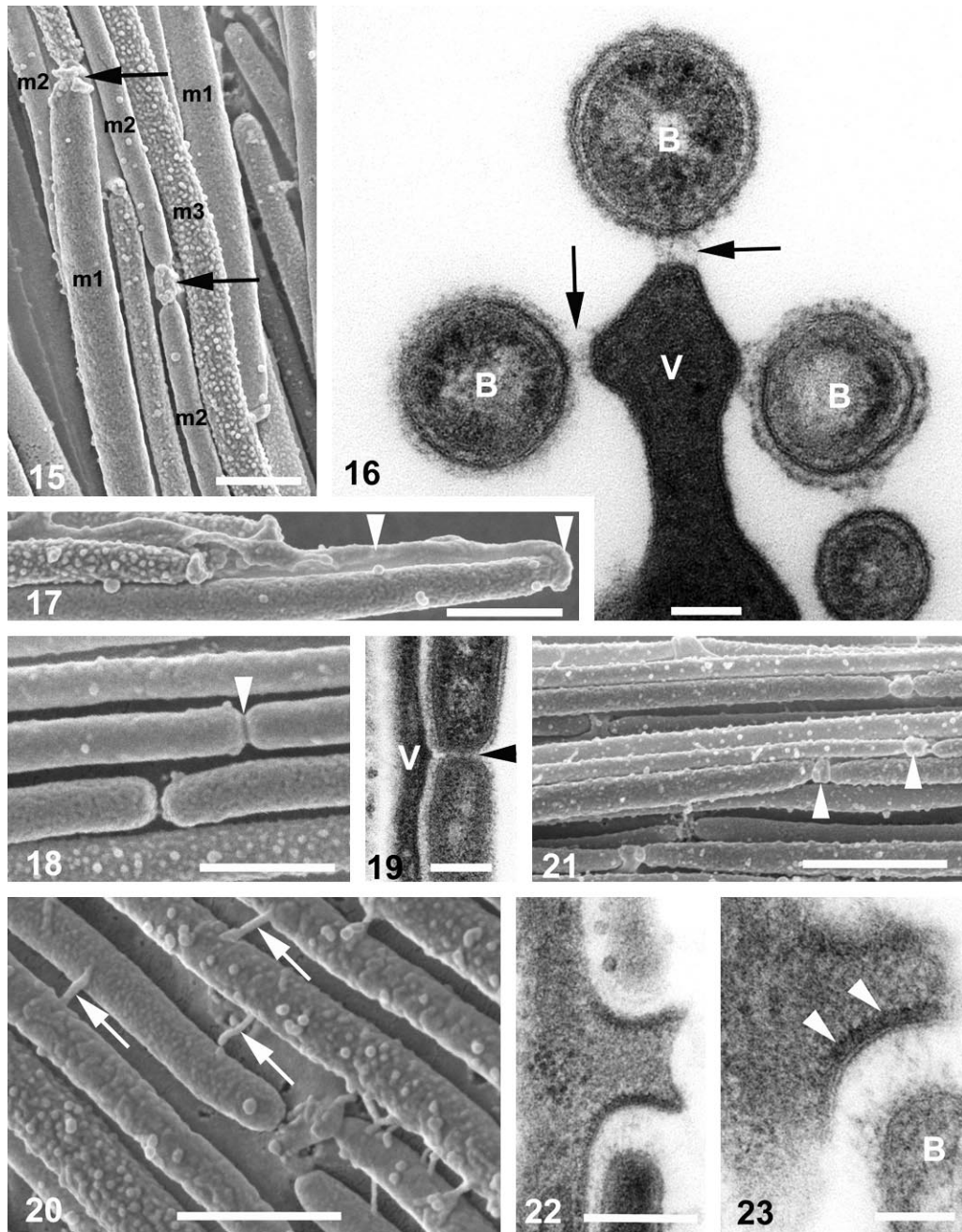
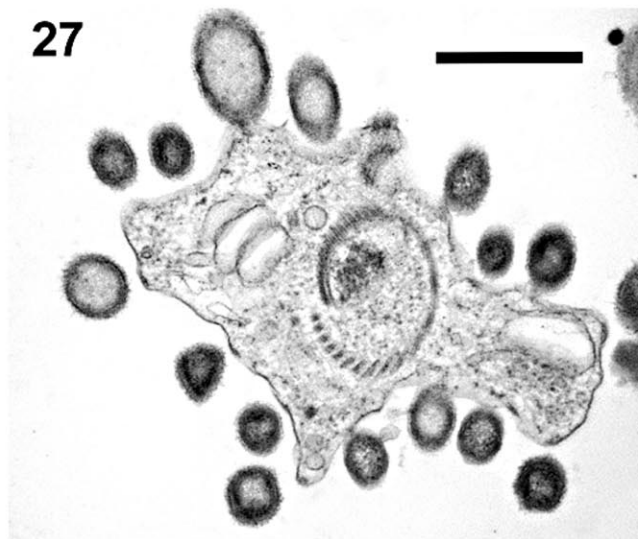
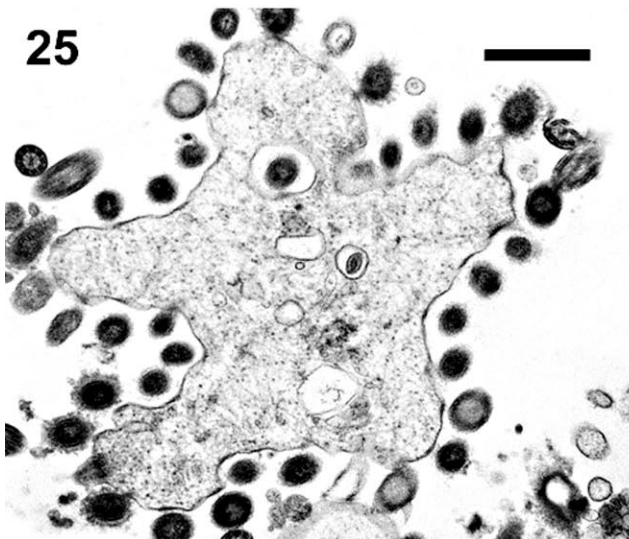
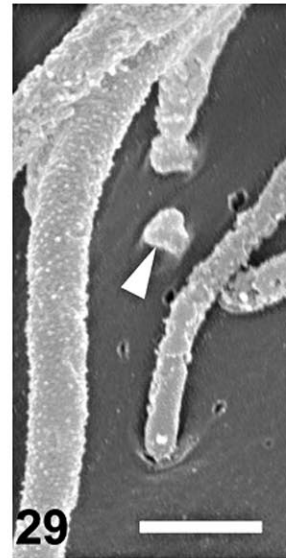
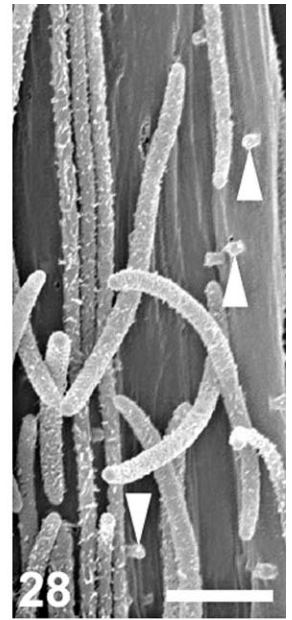
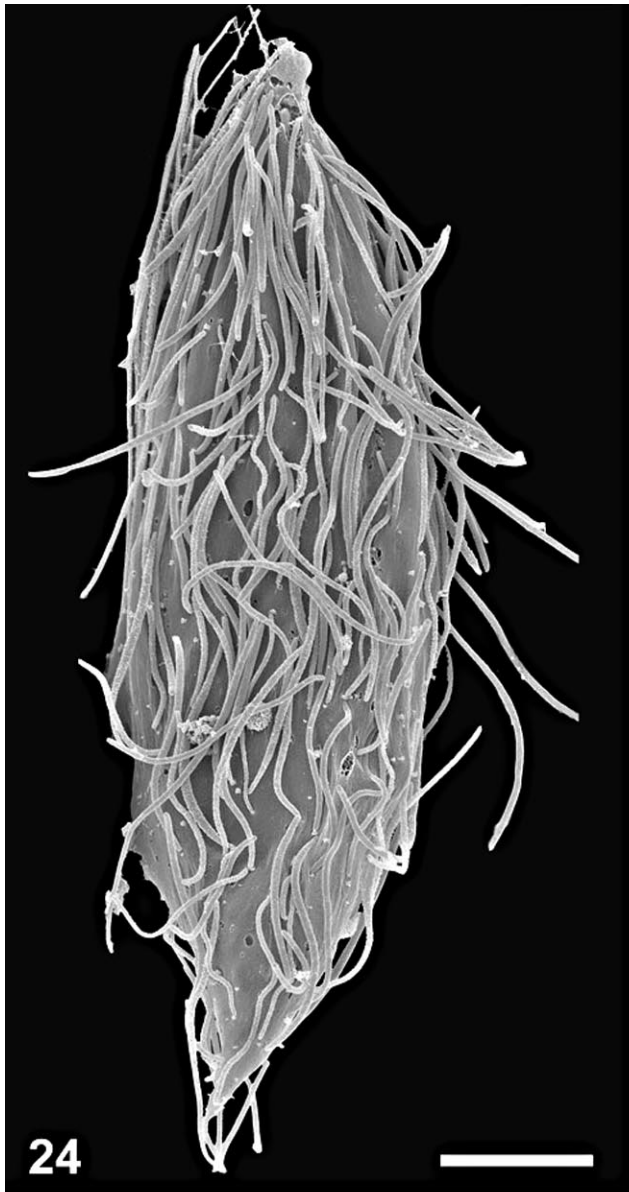


Fig. 15–23. Epibiotic bacteria on *Streblomastix strix* and associated cell-cell junctions. 15. SEM showing three morphotypes of epibiotic bacteria (m1, m2, and m3); arrows mark host protuberances or 'knobs' that articulate with the termini of the elongated bacteria (Bar = 0.5 μm). 16. TEM of the distal edge of a vane (V) showing the glycocalyx-like material or 'fuzz' (arrows) connecting the epibiotic bacteria (B) to the host cell (Bar = 0.1 μm). 17. SEM of the posterior end of the host cell showing the host cytoplasm (arrowheads) cupping the last epibiotic bacterium (Bar = 0.5 μm). 18. SEM showing septum formation (arrowhead) in a dividing bacterium (Bar = 0.5 μm). 19. TEM showing the septum (arrowhead) in a dividing bacterium that is affixed to a vane (V) (Bar = 0.25 μm). 20. SEM showing pili (arrows) between adjacent bacteria (Bar = 0.5 μm). 21. SEM showing host protuberances or 'knobs' (arrowheads) functioning as cell-cell junctions with the termini of epibiotic bacteria (Bar = 1 μm). 22. TEM through a junction illustrated in Fig. 21 showing their biconcave morphology (Bar = 0.25 μm). 23. TEM through a junction illustrated in Fig. 21 showing dark (osmophilic) material subtending the plasma membrane and glycocalyx-like material connecting the bacterium to the host (Bar = 0.1 μm).

Fig. 24–29. Surface features of *Streblomastix strix* following treatment with the antibiotic carbenecillin. 24. SEM showing a transitional stage in bacterial detachment and host cell reorganization (Bar = 5 μm). 25. TEM transverse section through a cell like the one shown in Fig. 24 showing aberrant bulges indicative of the normal stellate morphology in Fig. 2 (Bar = 1 μm). 26. SEM of a teardrop-shaped cell after three days of carbenecillin treatment (Bar = 2.5 μm). 27. TEM transverse section through a teardrop-shaped cell (Bar = 1 μm). 28, 29. High magnification SEMs show the isolated knobs (arrowheads) characteristic of transitional stages of bacterial detachment (Bar = 1 and 0.5 μm , respectively).



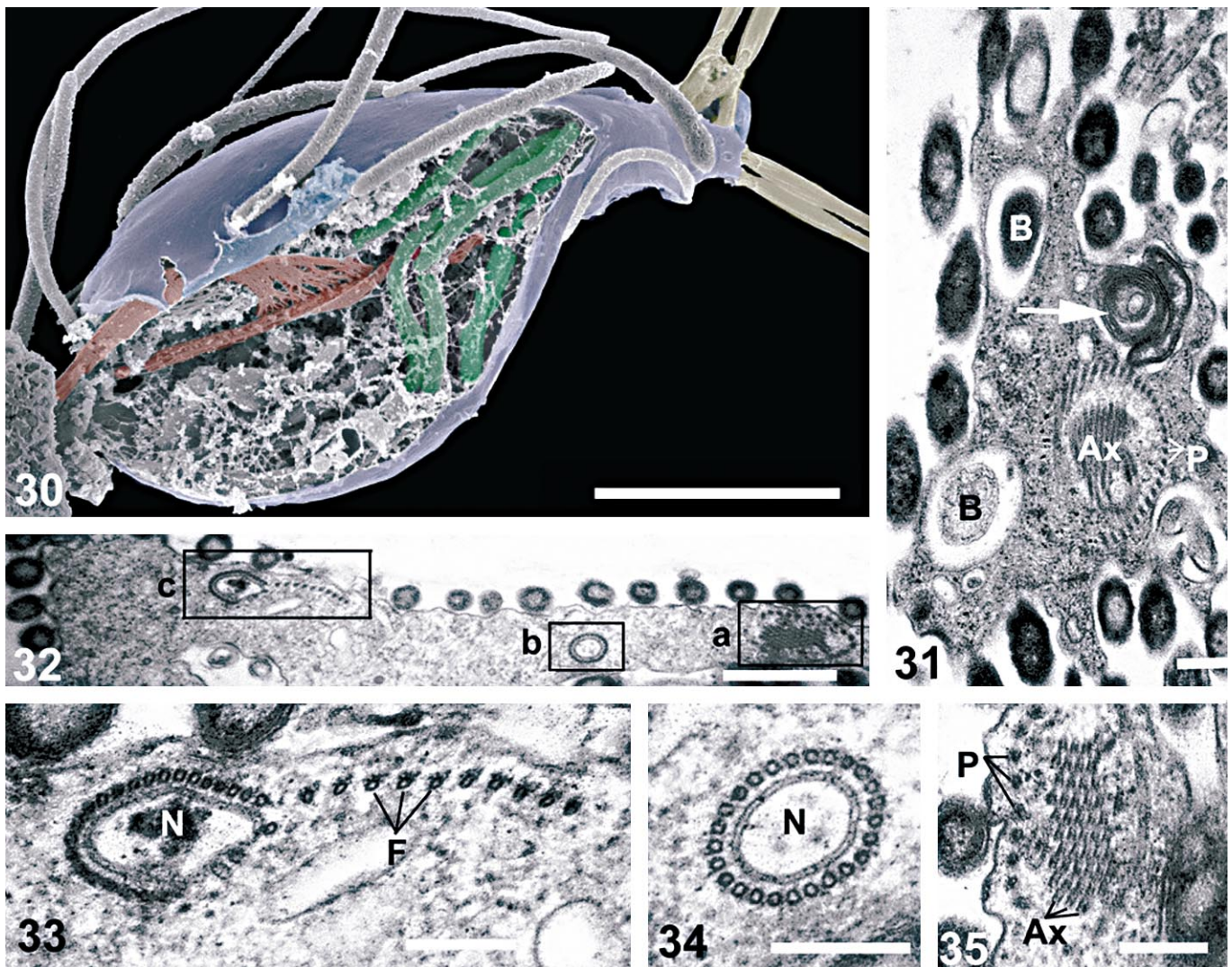


Fig. 30–35. Internal features of *Streblomastix strix* following treatment with the antibiotic carbenecillin. **30.** SEM of a teardrop-shaped cell with a portion of the plasma membrane (blue) removed and the four flagella (tan) oriented to the right. The axial cytoskeleton (red) bifurcated near the mid-region of the cell, and elongated intracellular bacteria (green) were present in the anterior region of the cell (Bar = 5 μm). **31.** TEM transverse section through the anterior region of a teardrop-shaped cell showing the pre-nuclear axostyle (Ax), microtubules of the pelta (P), a multilayered membranous structure of undetermined homology (arrow), and intracellular bacteria (B) (Bar = 0.5 μm). **32.** TEM oblique section through a teardrop-shaped cell showing three transverse views of the axial cytoskeleton (anterior end of cell to the right): 'box a' is shown in Fig. 35, 'box b' is shown in Fig. 34 and 'box c' is shown in Fig. 33 (Refer to Fig. 14D for a schematic of the plane of section) (Bar = 1 μm). **33.** The posterior region of the axial cytoskeleton shows a 'fan' of microtubules (F) branching away from the central axostylar cylinder containing the nucleus (N) (Bar = 0.25 μm). **34.** The mid-region of the axial cytoskeleton shows a tight cylinder of axostylar microtubules surrounding a long thread-like nucleus (N) (Bar = 0.25 μm). **35.** The anterior region of the axial cytoskeleton shows the pre-nuclear axostyle (Ax) and microtubules of the pelta (P) (Bar = 0.25 μm).

Following carbenecillin treatment, the cells of *S. strix* became teardrop-shaped and the axostyle changed significantly in structure. The branching fan of microtubules in carbenecillin-treated cells is probably a physical manifestation of 'telescoping', which resulted when the long spindle-shaped cell reduced in length to the teardrop shape. While the present highly derived form of *S. strix* is quite unlike any other oxymonads, the teardrop morphology of treated *S. strix* cells is reminiscent of other oxymonad shapes, such as *Monocercomonoides* and *Polymastix* (Brugerolle and Lee 2000).

The vanes lack microtubules altogether, and either the epibiotic bacteria function as an extracellular skeleton that structurally (or osmotically) supports vane morphology (Dexter-

Dyer and Khalsa 1993) or the host provides non-microtubular cytoskeletal support for the vanes. Nonetheless, the disappearance of vanes, bacterial attachment sites, and bacteria in carbenecillin-treated cells are all correlated, but specific relationships of cause and effect are not yet clear. The bacterial attachment sites or knobs are unique to *S. strix* and have a biconcave shape that accommodates the termini of two adjacent bacteria lying in the same longitudinal axis. These cell-cell junctions appear to be distributed haphazardly over the vanes and, aside from the anterior end of the cell and the flagella, are the only visible parts of the cell surface. The absence of bacteria on the anterior end of the cell almost certainly has functional advantages, because this region is more 'morpho-dynamic' than

the rest of the cell; its shape must change dramatically during holdfast formation, and during alterations in flagellar orientation, both of which would destabilize attached bacteria.

A mutualistic symbiosis? The adaptations to bacterial attachment in *S. strix* build a strong case for some mutually beneficial association between it and at least some of the bacteria. During antibiotic treatment, the bacteria were lost and the adaptations to bacterial attachment degenerated; *S. strix* was also unable to survive for more than a few days. This correlation is consistent with the health of *S. strix* being dependent on the health of its epibiotic bacteria. If *S. strix* and the bacteria are engaged in a mutually beneficial symbiosis, then what is its basis?

There are several possible explanations for this symbiosis, and it is important to keep in mind that the function of the bacteria need not be limited to a single role. For instance, the bacteria and *S. strix* might be engaged in a nutritional symbiosis, as has been inferred in several other symbioses in low-oxygen environments (e.g. Bernhard et al. 2000; Fenchel and Finlay 1989, 1991; Ott et al. 1998). In this scenario, the surface bacteria and *S. strix* cooperate by exchanging nutrients, benefiting from the products of one another's metabolism. The attachment sites and rigidity of *S. strix* could be to ensure a secure association with the bacteria, whilst the vanes would provide increased surface contact with the bacteria to facilitate the exchange of metabolites. Alternatively, Dexter-Dyer and Khalsa (1993) have argued that the bacteria play a chemosensory role, and that the specialized cell-cell junctions facilitate the relay of sensory information (e.g. bacterial membrane potentials) from epibiotic bacteria to *S. strix*. As *S. strix* swims, it may cover relatively large distances and enter environments with significantly different properties, which could be detected by the bacteria. This scheme, however, is difficult to reconcile with bacterial chemotaxis, because bacteria do not sense gradients in space, but rather in time (Armitage 1999).

While a number of characteristics and correlations are now clear, there are still a several unanswered questions surrounding the morphology of *S. strix* and its surface symbionts. Perhaps most obviously, the unusual length of the bacteria continues to beg an explanation. Although a role in the structural support of vanes is plausible, the length of the bacteria may be advantageous for other functions as well. Similarly, the functional significance and phylogenetic relationships of the three different bacterial morphotypes is totally unknown. It is possible that some of these morphotypes are participating in a symbiotic activity whilst others are clinging on as commensals. Additionally, possible functional roles (if any) of the intracellular bacteria remain unclear. What is clear, however, is that *S. strix* has accumulated several innovations associated with an extremely intimate symbiosis and the exploitation of low-oxygen environments.

ACKNOWLEDGMENTS

B. S. L. was supported by the National Science Foundation (Postdoctoral Research Fellowship in Microbial Biology, USA) and is a scholar of the CIAR, Program in Evolutionary Biology. P. J. K. is a Scholar of the CIAR, CIHR, and Michael Smith Foundation for Health Research. This work was funded by a grant (227301-00) from the Natural Sciences and Engineering Research Council of Canada (NSERC).

LITERATURE CITED

Armitage, J. P. 1999. Bacterial tactic responses. *Adv. Micro. Physiol.*, **41**:229–289.

Beams, H. W., King, R. L., Tahmisian, T. N. & Devine, R. 1960. Elec-

tron microscope studies on *Lophomonas striata* with special reference to the nature and position of the striations. *J. Protozool.*, **7**:91–101.

Bernhard, J. M., Buck, K. R., Farmer, M. A. & Bowser, S. S. 2000. The Santa Barbara Basin is a symbiosis oasis. *Nature*, **403**:77–80.

Bloodgood, R. A. & Miller, K. R. 1974. Freeze fracture of microtubules and bridges in motile axostyles. *J. Cell Biol.*, **62**:660–671.

Bloodgood, R. A., Miller, K. R., Fitzharris, T. P. & McIntosh, J. R. 1974. The ultrastructure of *Pyrrsonympha* and its associated microorganisms. *J. Morph.*, **143**:77–106.

Brugerolle, G. 1991. Flagellar and cytoskeletal systems in amitochondrial flagellates: Archamoeba, Metamonada and Parabasala. *Proto-plasma*, **164**:70–90.

Brugerolle, G. & König, H. 1997. Ultrastructure and organization of the cytoskeleton in *Oxymonas*, an intestinal flagellate of termites. *J. Eukaryot. Microbiol.*, **44**:305–313.

Brugerolle, G. & Lee, J. J. 2000. Order Oxymonadida. In: Lee, J. J., Leedale, G. F. & Bradbury, P. (ed.), *An Illustrated Guide to the Protozoa*. Allen Press Inc., Lawrence, KS. p. 1186–1195.

Brugerolle, G. & Patterson, D. 1997. Ultrastructure of *Trimastix convexa* Hollande, an amitochondriate anaerobic flagellate with a previously undescribed organization. *Europ. J. Protistol.*, **33**:121–130.

Cavalier-Smith, T. 1983. A 6-kingdom classification and a unified phylogeny. In: Schenk, H. E. A. & Schwemmler, W. (ed.), *Endocytobiology II*. Walter de Gruyter, Berlin. p. 1027–1034.

Cavalier-Smith, T. 1987. Eukaryotes with no mitochondria. *Nature*, **326**:332–333.

Cleveland, L. R. 1925. The effects of oxygenation and starvation on the symbiosis between the termite *Termopsis* and its intestinal flagellates. *Biol. Bull.*, **48**:309–325.

Dacks, J. B., Silberman, J. D., Simpson, A. G. B., Moruya, S., Kudo, T., Ohkuma, M. & Redfield, R. 2001. Oxymonads are closely related to the excavate taxon *Trimastix*. *Mol. Biol. Evol.*, **18**:1034–1044.

Dexter-Dyer, B. & Khalsa, O. 1993. Surface bacteria of *Streblomastix strix* are sensory symbionts. *BioSystems*, **31**:169–180.

Fenchel, T. & Finlay, B. J. 1989. *Kentrophoros*—a mouthless ciliate with a symbiotic kitchen garden. *Ophelia*, **30**:75–93.

Fenchel, T. & Finlay, B. J. 1991. The biology of free-living anaerobic ciliates. *Europ. J. Protistol.*, **26**:201–215.

Hollande, A. & Caruette-Valentin, J. 1970. La lignee des Pyrrsonymphines et les caracteres infrastructuraux communs aux genres *Opisthomonas*, *Oxymonas*, *Saccinobaculus*, *Pyrrsonympha*, et *Streblomastix*. *Compt. rend. Acad. Sci. (ser. D)*, **270**:1587–1590.

Keeling, P. J. & Leander, B. S. 2003. Characterisation of a non-canonical genetic code in the oxymonad *Streblomastix strix*. *J. Mol. Biol.*, **326**:1337–1349.

Kidder, G. W. 1929. *Streblomastix strix*, morphology and mitosis. *Univ. Calif. Publ. Zool.*, **33**:109–124.

Kofoid, C. A. & Swezy, O. 1919. Studies on the parasites of the termites. I. On *Streblomastix strix*, a polymastigote flagellate with a linear plasmodial phase. *Univ. Calif. Publ. Zool.*, **20**:21–40.

Kuznetsov, S. A., Langford, G. M. & Weiss, D. G. 1992. Actin-dependent organelle movement in squid axoplasm. *Nature*, **356**:722–725.

McIntosh, J. R. 1973. The axostyle of *Saccinobaculus*. II. Motion of the microtubule bundle and a structural comparison of straight and bent axostyles. *J. Cell Biol.*, **56**:304–323.

Moriya, S., Dacks, J. B., Takagi, A., Noda, S., Ohkuma, M., Doolittle, W. F. & Kudo, T. 2003. Molecular phylogeny of three oxymonad genera: *Pyrrsonympha*, *Dinenympha* and *Oxymonas*. *J. Eukaryot. Microbiol.*, **50**:190–197.

O'Kelly, C. J., Farmer, M. A. & Nerad, T. A. 1999. Ultrastructure of *Trimastix pyriformis* (Klebs) Bernard et al.: Similarities of *Trimastix* species with retortamonad and jakobid flagellates. *Protist*, **150**:149–162.

Ott, J. A., Bright, M. & Schiemer, F. 1998. The ecology of a novel symbiosis between a marine peritrich ciliate and chemoautotrophic bacteria. *Mar. Ecol.*, **19**:229–243.

Patterson, D. 1999. The diversity of eukaryotes. *Am. Nat.*, **154**:96–124.

Rother, A., Radek, R. & Hausmann, K. 1999. Characterization of surface structures covering termite flagellates of the family Oxymonadidae and ultrastructure of two oxymonad species, *Microrhopalodina multinucleata* and *Oxymonas* sp. *Europ. J. Protistol.*, **35**:1–16.

Simpson, A. G. B., Bernard, C. & Patterson, D. 2000. The ultrastructure

- of *Trimastix marina* Kent, 1880 (Eukaryota), an excavate flagellate. *Europ. J. Protistol.*, **36**:229–252.
- Simpson, A. G. B., Radek, R., Dacks, J. B. & O’Kelly, C. J. 2002. How oxymonads lost their groove: an ultrastructural comparison of *Monocercomonoides* and excavate taxa. *J. Eukaryot. Microbiol.*, **49**: 239–248.
- Stingl, U. & Brune, A. 2003. Phylogenetic diversity and whole-cell hybridization of oxymonad flagellates from the hindgut of the wood-feeding lower termite *Reticulitermes flavipes*. *Protist*, **154**:147–155.
- Trager, W. 1934. The cultivation of a cellulose-digesting flagellate, *Trichomonas termopsidis*, and of certain other termite protozoa. *Biol. Bull.*, **66**:82–190.
- Yamin, M. A. 1979. Scanning electron microscopy of some symbiotic flagellates from the termite *Zootermopsis*. *Trans. Amer. Micros. Soc.*, **98**:276–279.

Received 10/23/03, 11/11/03, 02/18/04; accepted 02/19/04